

# Microstructure and Properties of a Deformation-Processed Cu-Cr-Ag In Situ Composite by Directional Solidification

Keming Liu, Deping Lu, Haitao Zhou, Yanling Yang, Andrej Atrens, and Jin Zou

(Submitted December 25, 2012; in revised form March 22, 2013; published online September 11, 2013)

Cu-7Cr-0.07Ag alloys were prepared by casting and directional solidification, from which deformation-processed in situ composites were prepared by thermo-mechanical processing. The microstructure, mechanical properties, and electrical properties were investigated using optical microscopy, scanning electronic microscopy, tensile testing, and a micro-ohmmeter. The second-phase Cr grains of the directional solidification Cu-7Cr-0.07Ag in situ composite were parallel to the drawing direction and were finer, which led to a higher tensile strength and a better combination of properties.

**Keywords** Cu-Cr-Ag, directional solidification, in situ composite, microstructure, property

## 1. Introduction

The rapid development of the electric, microelectronic, energy, and transport industries has increased property requirements, so that conductors need to possess good conductivity and high strength, and be available at a reasonable cost. As a consequence, there has been extensive research (Ref 1-5) on deformation-processed Cu-based in situ composites (such as Cu-Ag, Cu-Nb-Ag, Cu-Fe-Ag, and Cu-Cr-Ag) due to their excellent strength and good conductivity. Recent research (Ref 6, 7) has shown that the three most important approaches to improve strength and conductivity of these in situ composites are (i) heavy hot and cold working, (ii) intermediate heat treatment (IHT), and (iii) complex alloying. Heavy hot and cold working transforms the dendrites in the as-cast ingot into fibers that provide the strengthening for obtaining high strength. IHT for an appropriate time at an appropriate temperature allows high conductivity to be achieved. Optimized complex alloying produces an excellent combination of strength and conductivity. However, there are few reports that have investigated the possibility of improving the properties of in situ composites by controlling the microstructure of the as-cast starting ingot.

Microstructure is an important factor influencing the final properties (Ref 8). An increasing interest has been devoted to improving mechanical and physical properties by producing the optimum microstructure (Ref 9, 10). Directional solidification

**Keming Liu, Deping Lu, Yanling Yang, and Jin Zou**, Jiangxi Key Laboratory for Advanced Copper and Tungsten Materials, Jiangxi Academy of Sciences, Nanchang 330029, People's Republic of China; **Haitao Zhou**, School of Materials Science and Engineering, Central South University, Changsha 410083, People's Republic of China; and **Andrej Atrens**, The University of Queensland, Brisbane, QLD 4072, Australia. Contact e-mail: [jokeyliu@163.com](mailto:jokeyliu@163.com).

(DS) is one of the most widely used techniques which produce high quality components, as it permits a precise control of the temperature gradient and drawing velocity to obtain a desirable microstructure (Ref 2, 11). The Bridgman DS technique was established in the 1920s as the foundation of modern DS and single-crystal growth techniques. Subsequently, many DS variations have been developed and applied to the manufacture of high quality materials, such as semiconductor materials, magnetic functional materials, and composites, since they can control the growth direction of crystals and can effectively eliminate transverse grain boundaries. These techniques have made significant contributions to achieving ultrafine columnar crystals and to investigating solidification mechanisms.

In our previous work (Ref 12), we investigated the microstructure and properties of deformation-processed Cu-Cr-Ag in situ composites produced from conventional cast ingots. This paper builds on that work and studies the influence of DS on the microstructure and the properties of a deformation-processed Cu-Cr-Ag in situ composite.

## 2. Experimental Details

The Cu-7Cr-0.07Ag alloy was produced by melting appropriate amounts of electrolytic Cu, commercial Cr, and Ag (of at least 99.94 wt.% purity) using a vacuum induction furnace. The molten alloy was cast into a graphite mold to produce rod-shaped ingots. The in situ composites were produced from the ingot by a series of hot deformation and cold deformation steps with IHTs (Ref 12). The cumulative cold deformation strain  $\eta = \ln(A_0/A_f)$ , where  $A_0$  was the original cross-sectional area and  $A_f$  was the final cross-sectional area.

DS was carried out using a Bridgeman-type apparatus under the protection of high purity argon at 380 Pa. Specimens of Cu-7Cr-0.07Ag, typically 6.8 mm in diameter and 100 mm in length, were cut from the cast ingot and placed into an alumina crucible, which had been coated with yttria to separate the alloy and the crucible. The alloy was melted, homogenized by holding for 20 min, and directionally solidified at a velocity of

150  $\mu\text{m/s}$ . Figure 1(a) and (b) presents schematic and section diagrams of the DS equipment. The molten alloy is pulled downward by the pulling rod and pulling motor, and cooled by the liquid metal coolant. The graphite cannula between the aluminum oxide tube and the inductor is used to provide radiant heat to the molten alloy due to its good conductivity and to reduce the influence of electromagnetic fields on the thermo-couple thermometer.

The preparation of DS deformation-processed in situ composites was similar to that used previously (Ref 12), meaning the DS specimens were (i) solution treated at 950  $^{\circ}\text{C}$  for 3 h, (ii) cold rolled to  $\eta = 1.7$ , and (iii) wire drawn and subjected to intermediate hear treatment (IHT) as follows: cold drawn (CD) from  $\eta = 1.7$  to 3.1; IHT at 550  $^{\circ}\text{C}$  for 30 min; CD to  $\eta = 4.7$ ; IHT at 550  $^{\circ}\text{C}$  for 20 min; CD to  $\eta = 6.6$ ; IHT at 650  $^{\circ}\text{C}$  for 10 min; and CD to  $\eta = 8$ .

The above IHT times and temperatures were found experimentally to be optimum. The IHT provides partial softening without recrystallization. It was found experimentally that grain coarsening (leading to poor final properties) occurred if the IHT temperature was too high and the IHT time too long. Furthermore, it was found to be not beneficial to carry out the next cold deformation if the IHT was at too low a temperature and too short a duration.

The diameters of the alloy were 0.95, 0.67, 0.35, 0.26, and 0.13 mm for the following cumulative cold deformation strains  $\eta = 4, 4.7, 6, 6.6,$  and 8, respectively.

The microstructures of the as-cast and deformation-processed specimens were investigated using an optical microscope (Leica DMI5000 M) and a scanning electronic microscope (SEM/JSM-6360LV). The SEM specimens were prepared by standard mechanical polishing and were etched in a solution of 120 mL  $\text{H}_2\text{O}$ , 20 mL  $\text{HCl}$ , and 5 g  $\text{FeCl}_3$ .

Tensile tests of the deformation-processed specimens were conducted at room temperature using an electronic tensile testing machine (EMT2203-B) equipped with an extensometer and using custom-designed wire grips. The strain rate was  $1.5 \times 10^{-4}/\text{s}$ . At least three specimens were tested at each cold deformation strain. Figure 2 presents the external appearance of the wire grips. The surface of the alloy wire grip was covered with a layer of rubber, which reduced the stress concentration

and increased the frictional force between the in situ composite wire and the wire grips.

Electrical resistivity,  $\rho$ , was measured at room temperature using a ZY9987 digital micro-ohmmeter with precision of 1  $\mu\Omega$ . The corresponding conductivity was evaluated according to the definition of the International Annealed Copper Standard (ICAS) in which 1.7241  $\mu\Omega \text{ cm}$  is defined as 100 % IACS.

### 3. Results

#### 3.1 Microstructure

Figure 3 presents the microstructure of cast and DS Cu-7Cr-0.07Ag alloys. Figure 3(a) shows that the second-phase Cr dendrites were embedded in the Cu matrix, and were randomly oriented with respect to the ingot axis in the cast alloy, which is in agreement with prior studies (Ref 12-14). The size, shape, and distribution of second-phase Cr grains were significantly different in the material processed from a DS ingot, as shown in Fig. 3(b). The Cr grains of the DS Cu-7Cr-0.07Ag alloy were

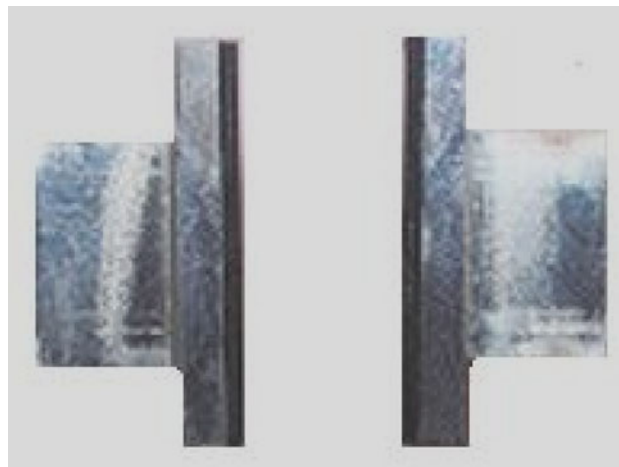


Fig. 2 The external appearance of the wire grips

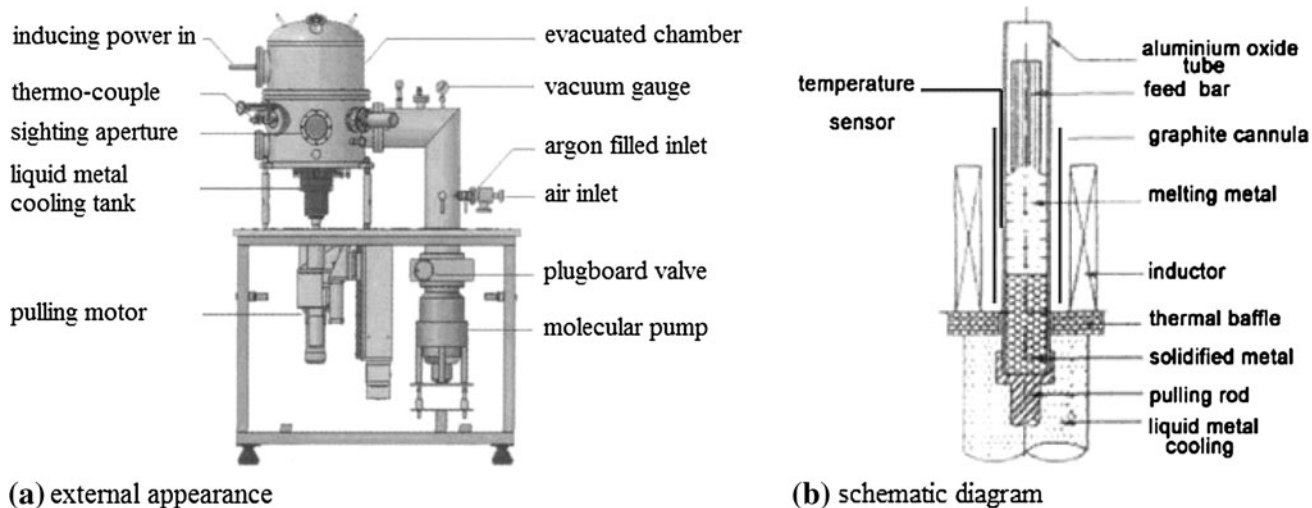
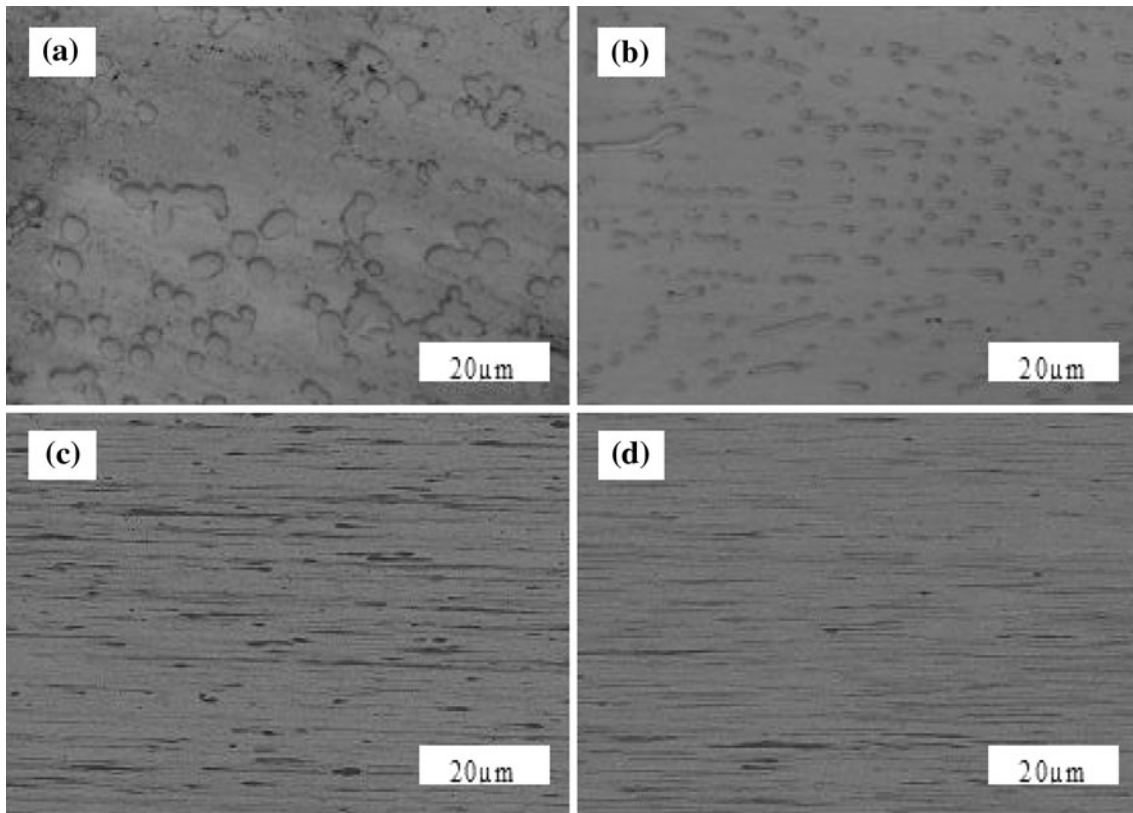


Fig. 1 Directional solidification equipment



**Fig. 3** Microstructures: (a) longitudinal section of cast Cu-7Cr-0.07Ag alloy, (b) longitudinal section of DS Cu-7Cr-0.07Ag alloy, (c) longitudinal section of cast Cu-7Cr-0.07Ag in situ composite with  $\eta = 8$ , and (d) longitudinal section of DS Cu-7Cr-0.07Ag in situ composite with  $\eta = 8$

finer and more uniform than those of the cast alloy, and formed thin Cr fiber-like grains parallel to the drawing direction. This is attributed to the DS technique, which produced a strict one-dimensional thermal flux along the sample axis and sufficient heat exchange between the sample and cooling medium by an appropriate temperature gradient and drawing velocity. Figure 3(c) and (d) presents typical microstructures of longitudinal sections of the deformation-processed in situ composites with a cumulative cold deformation strain  $\eta = 8$  for cast and DS Cu-7Cr-0.07Ag ingots respectively. These show the Cu matrix and thin Cr fibers parallel to the drawing direction. The Cr fibers in the in situ composite from the DS ingot were finer and evenner than those from the cast ingot. This is also attributed to the DS technique, which produced a finer and more uniform Cr phase, and formed Cr fibers elongated parallel to the drawing direction.

To characterize the second Cr-rich phase, EDS analysis was used at higher magnification SEM observations. The results are shown in Fig. 4, which indicates that the mass percent of Cr was 95.45%, whereas the mass percent of Cu was only 4.55%. There is no an intermetallic compound between Cu and Cr. When the selected areas are not sufficiently large, their composition is difficult to measure accurately using EDS because the EDS signal comes from a significant interaction volume. Therefore, it can be concluded that the second phase is largely Cr.

### 3.2 Tensile Strength

Figure 5 presents the tensile strength plotted for convenience against cumulative cold deformation strain for the deformation-processed in situ composites with two IHTs from cast and DS Cu-7Cr-0.07Ag alloys. The IHTs provide partial

softening as suggested above. The tensile strength of each in situ composite increased with increasing strain. Previous studies revealed that the strength of the deformation-processed Cu-based in situ composites obeys the Hall-Petch correlation (Ref 15):

$$\sigma = \sigma_0 + k\lambda^{-1/2}, \quad (\text{Eq 1})$$

where  $\sigma$  is the tensile strength,  $\sigma_0$  the stress required to move dislocations in the matrix and fibers, and  $\lambda$  the average spacing between fibers. Cold deformation, with a large deformation strain, transformed the as-cast microstructure into an in situ composite. The increase in tensile strength with increasing cold deformation strain is attributed to the decrease of average spacing between fibers, i.e., the tensile strength obeys the Hall-Petch correlation and is determined by the fiber spacing. The tensile strength of the DS Cu-7Cr-0.07Ag was much higher than those from the cast ingot at the same cold deformation strain. At  $\eta = 8$ , the increase in tensile strength was almost 300 MPa. The higher tensile strength of DS Cu-7Cr-0.07Ag is attributed to the DS technique, which made the Cr grains finer and more uniform, promoted the directional alignment of the Cr phase, and resulted in smaller fiber spacing at the same  $\eta$ . The tensile strength decreased after IHTs, maybe due to the recovery and recrystallization of the composites (Ref 16-18).

### 3.3 Conductivity

Figure 6 presents the conductivity versus cumulative cold deformation strain for the deformation-processed in situ composites with two IHTs from cast and DS Cu-7Cr-0.07Ag alloys.

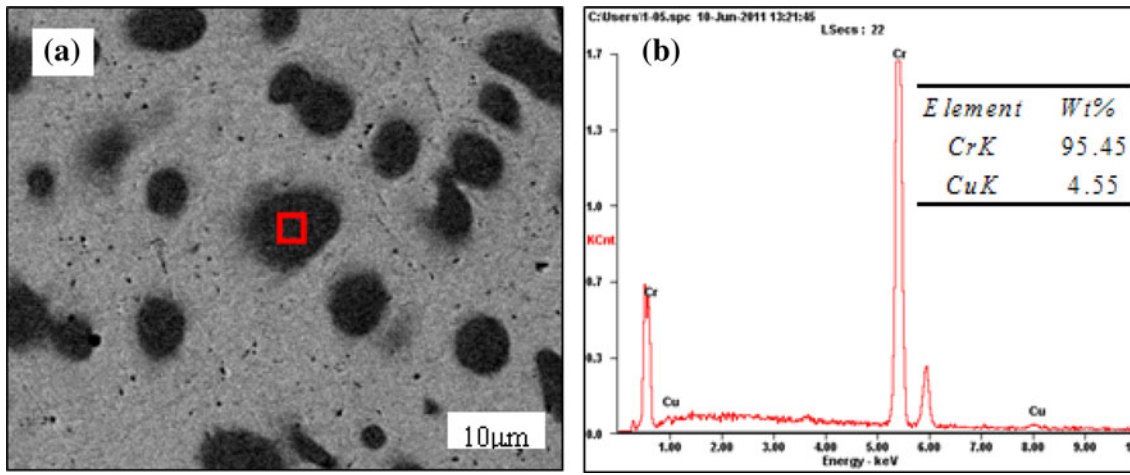


**Fig. 4** SEM morphology and EDS analysis: (a) SEM morphology of Cu-7Cr-0.07Ag alloy and (b) EDS analysis of the second phase

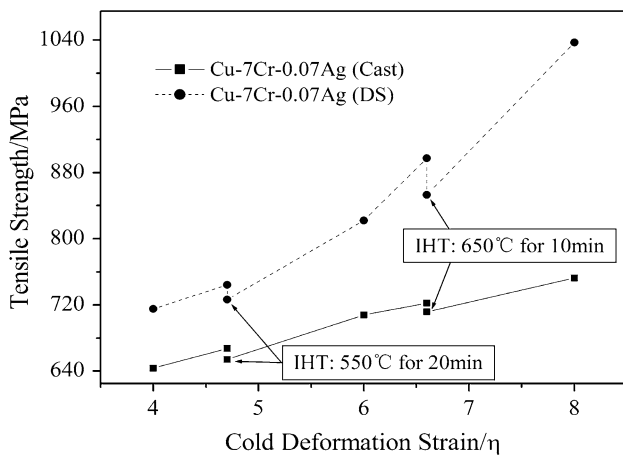


**Fig. 5** Tensile strength of cast and DS Cu-7Cr-0.07Ag with different deformations and intermediate heat treatments vs. cold deformation strain

For both the cast and DS deformation-processed Cu-7Cr-0.07Ag in situ composites, the conductivity decreased with increasing cumulative cold deformation strain. The conductivity increased after each IHT and then decreased gradually with further cold deformation, which was in agreement with the prior studies for the deformation-processed Cu-based in situ composites (Ref 18, 19). In addition, for each cumulative cold deformation strain, the conductivity of the deformation-processed Cu-7Cr-0.07Ag in situ composite from DS alloys was slightly lower than those from the cast ingots

#### 4. Discussion

Figure 6 shows that the conductivity of both DS and cast deformation-processed in situ composites decreased with increasing strain, and the conductivity of DS Cu-7Cr-0.07Ag was slightly lower than that of the cast alloy at the same cold deformation strain. This is not to imply that there is a causal relationship among these parameters. In fact, the conductivity is determined by the microstructure and composition of the constituent phases as described in the following.

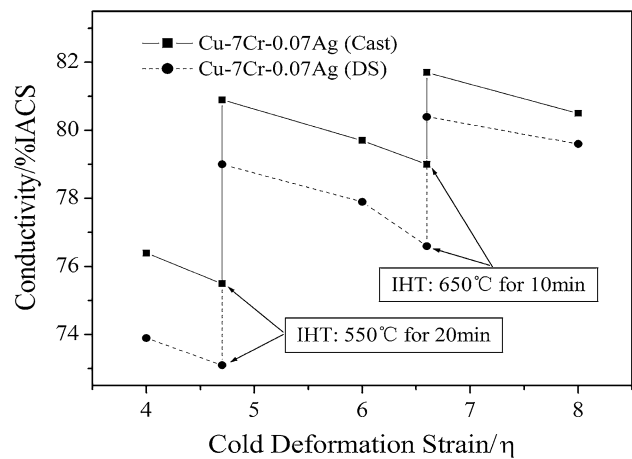


**Fig. 6** Conductivity of cast and DS Cu-7Cr-0.07Ag with different deformations and intermediate heat treatments vs. cold deformation strain

The resistivity of the deformation-processed Cu-based in situ composites can be evaluated using a parallel-circuit model (Ref 20, 21):

$$1/\rho = f_{Cu}/\rho_{Cu} + f_{Cr}/\rho_{Cr}, \quad (\text{Eq 2})$$

where  $\rho_{Cu}$  and  $\rho_{Cr}$  are the resistivity of the Cu and Cr phase, respectively, and  $f_{Cu}$  and  $f_{Cr}$  are volume fractions of the Cu and Cr phase, respectively. The contribution to the total resistivity from the Cr fibers was similar for both composites because of the same volume fraction, i.e.,  $f_{Cr}$  was the same, and the resistivity of Cr is much higher than that of Cu. Therefore, the main difference of the two composites is attributed to the resistivity of copper matrix, which can be partitioned into the contribution of the four main scattering mechanisms (Ref 20):

$$\rho_M = \rho_{PHO} + \rho_{DIS} + \rho_{INT} + \rho_{IMP}, \quad (\text{Eq 3})$$

where  $\rho_M$  is the resistivity of copper matrix,  $\rho_{PHO}$  is the resistivity contribution from phonon scattering,  $\rho_{DIS}$  is dislocation scattering,  $\rho_{INT}$  is interface scattering, and  $\rho_{IMP}$  is impurity scattering. Composites with the same cold deformation strain have similar values of  $\rho_{PHO}$  and  $\rho_{DIS}$ . The  $\rho_{IMP}$  of the two in situ

composites was similar for the same component and volume fraction. The main differences in the measured resistivity came from different interface scatterings, i.e.,  $\rho_{\text{INT}}$ . The interfacial density of the composites increases with fiber refinement caused by increasing cold deformation strain, which results in increasing  $\rho_{\text{INT}}$ . Therefore, the conductivity of the in situ composites decreased. For the same reason, at the same cold deformation strain, the conductivity of DS Cu-7Cr-0.07Ag was slightly lower due to the finer fibers. The conductivities of both in situ composites increased after each IHT. This may be attributed to the fact that the IHTs promote Cr precipitation from the Cu matrix, which decreases the resistivity (Ref 22). In addition, recovery and recrystallization during IHTs also reduce the resistivity (Ref 16-18).

## 5. Conclusions

- (1) DS Cu-7Cr-0.07Ag alloy had aligned, finer, and even second-phase Cr grains than those of the as-cast Cu-7Cr-0.07Ag.
- (2) The cold-worked DS Cu-7Cr-0.07Ag in situ composite had Cr fibers finer than the cold-worked as-cast Cu-7Cr-0.07Ag in situ composite.
- (3) For each deformation strain, the tensile strength of the cold-worked DS Cu-7Cr-0.07Ag in situ composite was higher than that of the cold-worked as-cast Cu-7Cr-0.07Ag in situ composite, and the conductivity of the cold-worked DS Cu-7Cr-0.07Ag in situ composite was slightly lower than that of the cold-worked as-cast Cu-7Cr-0.07Ag in situ composite.
- (4) The higher tensile strength of the cold-worked DS Cu-7Cr-0.07Ag in situ composite is attributed to the finer microstructure.
- (5) The cold-worked DS Cu-7Cr-0.07Ag in situ composite with  $\eta = 8$  achieved a tensile strength of 1037 MPa and a conductivity of 79.6 % IACS compared with a tensile strength of 752 MPa and a conductivity of 80.4 % IACS for the cold-worked as-cast Cu-7Cr-0.07Ag in situ composite. The tensile strength was significantly improved, whereas there was only a small decrease in conductivity, which indicated that DS produced an in situ composite with significantly increased strength and improved combination of properties.

## Acknowledgments

This project was financially supported by the National Natural Science Foundation of China (No. 50961006), the Key Program of Natural Science Foundation of Jiangxi Province (No. 20133BAB20008), the Open Foundation of Jiangxi Key Laboratory for Advanced Copper and Tungsten Materials (No. 2011-TW-02, 2010-WT-01), and the Natural Science Foundation of Jiangxi Academy of Sciences (No. 2012-YQC-09).

## References

1. J.B. Liu, L. Zhang, and L. Meng, Effects of Rare-Earth Additions on the Microstructure and Strength of Cu-Ag Composites, *Mater. Sci. Eng. A*, 2008, **498**, p 392–396

2. D. Raabe, S. Ohsaki, and K. Hono, Mechanical Alloying and Amorphization in Cu-Nb-Ag In Situ Composite Wires Studied by Transmission Electron Microscopy and Atom Probe Tomography, *Acta Mater.*, 2009, **57**, p 5254–5263
3. Z.X. Xie, H.Y. Gao, Q. Lu, J. Wang, and B.D. Sun, Effect of Ag Addition on the As-Cast Microstructure of Cu-8 wt.% Fe In Situ Composites, *J. Alloys Compd.*, 2010, **508**, p 320–323
4. K.M. Liu, D.P. Lu, H.T. Zhou, A. Atrens, J. Zou, Y.L. Yang, and S.M. Zeng, Effect of Ag Micro-Alloying on the Microstructure and Properties of Cu-14Fe In-Situ Composite, *Mater. Sci. Eng. A*, 2010, **527**, p 4953–4958
5. X. Sauvage, P. Jessner, F. Vurpillot, and R. Pippan, Nanostructure and Properties of a Cu-Cr Composite Processed by Severe Plastic Deformation, *Scripta Mater.*, 2008, **58**, p 1125–1128
6. Y. Jin, K. Adachi, T. Takeuchi, and H.G. Suzuki, Ageing Characteristics of Cu-Cr In-Situ Composite, *J. Mater. Sci.*, 1998, **33**, p 1333–1341
7. L. Zhang, L. Meng, and J.B. Liu, Effects of Cr Addition on the Microstructural, Mechanical and Electrical Characteristics of Cu-6 wt.%Ag Microcomposite, *Scripta Mater.*, 2005, **52**, p 587–592
8. H. Fu, Z. Zhang, Y. Jiang, and J. Xie, Improvement of Magnetic Properties of an Fe-6.5 wt.% Si Alloy by Directional Solidification, *Mater. Lett.*, 2011, **65**, p 1416–1419
9. X.F. Ding, J.P. Lin, H. Qi, L.Q. Zhang, X.P. Song, and G.L. Chen, Microstructure Evolution of Directionally Solidified Ti-45Al-8.5Nb-(W, B, Y) Alloys, *J. Alloys Compd.*, 2011, **509**, p 4041–4046
10. L.S. Luo, Y.Q. Su, J.J. Guo, X.Z. Li, S.M. Li, H. Zhong, L. Liu, and H.Z. Fu, Peritectic Reaction and Its Influences on the Microstructures Evolution During Directional Solidification of Fe-Ni Alloys, *J. Alloys Compd.*, 2008, **461**, p 121–127
11. L. Liu, T. Huang, M. Qu, G. Liu, J. Zhang, and H. Fu, High Thermal Gradient Directional Solidification and Its Application in the Processing of Nickel-Based Superalloys, *J. Mater. Process. Technol.*, 2010, **210**, p 159–165
12. K.M. Liu, D.P. Lu, H.T. Zhou, A. Atrens, Z.B. Chen, J. Zou, and S.M. Zeng, Influence of Ag Micro-Alloying on the Microstructure and Properties of Cu-7Cr In Situ Composite, *J. Alloys Compd.*, 2010, **500**, p L22–L25
13. J.Q. Deng, X.Q. Zhang, S.Z. Shang, F. Liu, Z.X. Zhao, and Y.F. Ye, Effect of Zr Addition on the Microstructure and Properties of Cu-10Cr In Situ Composites, *Mater. Design*, 2009, **30**, p 4444–4449
14. Y. Liu, S. Shao, K.M. Liu, X.J. Yang, and D.P. Lu, Microstructure Refinement Mechanism of Cu-7Cr In Situ Composites with Trace Ag, *Mater. Sci. Eng. A*, 2012, **531**, p 141–146
15. H.Y. Gao, J. Wang, D. Shu, and B.D. Sun, Effect of Ag on the Microstructure and Properties of Cu-Fe In Situ Composites, *Scripta Mater.*, 2005, **53**, p 1105–1109
16. H.Y. Gao, J. Wang, D. Shu, and B.D. Sun, Effect of Ag on the Aging Characteristics of Cu-Fe In Situ Composites, *Scripta Mater.*, 2006, **54**, p 1931–1935
17. Z.W. Wu, J.J. Liu, Y. Chen, and L. Meng, Microstructure, Mechanical Properties and Electrical Conductivity of Cu-12 wt.% Fe Microcomposite Annealed at Different Temperatures, *J. Alloys Compd.*, 2009, **467**, p 213–218
18. J.P. Ge, H. Zhao, Z.Q. Yao, and S.H. Liu, Microstructure and Properties of Deformation-Processed Cu-Fe In-Situ Composites, *Trans. Nonferrous Met. Soc. China*, 2005, **15**, p 971–977
19. H.Y. Gao, J. Wang, D. Shu, and B.D. Sun, Microstructure and Properties of Cu-11Fe-6Ag In Situ Composite After Thermo-Mechanical Treatments, *J. Alloys Compd.*, 2007, **438**, p 268–273
20. S.I. Hong and M.A. Hill, Microstructure and Conductivity of Cu-Nb Microcomposites Fabricated by the Bundling and Drawing Process, *Scripta Mater.*, 2001, **44**, p 2509–2515
21. F. Heringhaus, D. Raabe, and G. Gottstein, On the Correlation of Microstructure and Electromagnetic Properties of Heavily Cold Worked Cu-20% Nb Wires, *Acta Metall. Mater.*, 1995, **43**, p 1467–1476
22. D. Raabe, K. Miyake, and H. Takahara, Processing, Microstructure, and Properties of Ternary High-Strength Cu-Cr-Ag In Situ Composites, *Mater. Sci. Eng. A*, 2000, **291**, p 186–197